



Hydrophobic Drug Release Studies from the Core/Shell Magnetic Mesoporous Silica Nanoparticles and their Anticancer Application

Amina Hussain*

Department of Environmental Sciences, Fatima Jinnah Women University, Rawalpindi

Abstract: Multiple therapeutic hydrophobic drugs can be delivered simultaneously by inorganic, biocompatible iron core mesoporous silica shell nanoparticles. We synthesized superparamagnetic iron oxide nanocrystals encapsulated within mesostructured silica spheres through the sol-gel process. The dose of hydrophobic drugs Paclitaxel (PTX) and Camptothecin (CPT) loading and released on $\text{Fe}_3\text{O}_4@\text{SiO}_2$ core/shell nanoparticle detected by U.V-visible spectrophotometry using a platform of nanoparticles (NPS). After being subjected to external heating, the drug release efficiency of paclitaxel (PTX) and camptothecin (CPT) $\text{Fe}_3\text{O}_4@\text{SiO}_2$ core/shell nanoparticles is increased. Paclitaxel (PTX) and Camptothecin (CPT) $\text{Fe}_3\text{O}_4@\text{SiO}_2$ core/shell nanoparticles did not heat the solution when an alternating magnetic field (AMF) was applied, and there was only mild drug leakage. When compared to $\text{Fe}_3\text{O}_4@\text{MSNs}$, the nanoparticles (PTX) and (CPT) $\text{Fe}_3\text{O}_4@\text{MSNs}$ function as cancer-targeting mediators, increasing the killing of PANC-1 cancer cells. Human cancer cells were given these therapeutic anticancer water-insoluble drugs with nanoparticles, which is a valuable vehicle for drug delivery, and induced the inhibition of proliferation. Therefore, the goal of this study to emphasize $\text{Fe}_3\text{O}_4@\text{SiO}_2$ core/shell potential as a superior candidate for hydrophobic drug delivery to the PANC-1 cancer cell.

Keywords: Mesoporous silica, nanoparticles, loading, release, hydrophobic drugs, PANC-1 cells

1. INTRODUCTION

The lack of appropriate biocompatible delivery mechanisms for most hydrophobic anticancer drugs is a big hurdle and threat for cancer treatment. Drugs water insolubility makes it difficult to administer drugs through the intravenous route, so improving aqueous solubility is especially necessary [1]. Although most essential anticancer agents have low water solubility, researchers have concentrated on finding a new delivery system for these molecules that do not rely on organic solvents. Nanoparticles have a lot of potentials and are an excellent means to transport anti-cancer drugs into certain organs or cell types, they've been intensively developed for use in cancer therapy [2]. Paclitaxel (PTX), a plant-derived alkaloid with cytotoxic effects in breast, prostate, and cervical cancers, is an anticancer drug. However, this alkaloid is not fully soluble in water [3, 4]. Camptothecin (CPT) is among the most successful anticancer drugs of the twenty-

first century. Even though studies have shown their efficacy against stomach, colon, throat, and prostate cancers, and also breast, lung cancers, and leukemia [5, 6].

Precision medicine, described as "the correct medicine, at the correct dose, at the accurate time, to the correct person," is a rapidly growing and influential cancer treatment practice around the world. Individual variability is taken into account in the design of customized disease care regimens in this new method [7]. The requirement of the correct therapeutic drug distribution at the desired time to the precise site of the disease, as well as the precise therapeutic dosage, poses a trial [8-11]. Over the last decade, many examples of drug-delivery stimuli-responsive platforms have been created, including those that respond to cellular internal stimuli (change in pH or bio compounds), as well as external stimuli such as (ultrasound, heat, and light) [11-15].

Progress in using inorganic nanoparticles for biological means has accelerated due to the wide volume of work completed in material modification. These nanoscale materials provide a strong framework that can be used for a variety of purposes [15-16]. Mesoporous magnetic materials have a wide range of uses in industry and research [17]. Magnetic resonance imaging contrast enhancement, drug delivery, heat, or hyperthermia are only a few of the biomedical uses for superparamagnetic nanoparticles that have been studied extensively. Drug delivery triggered by heat produced when magnetic nanoparticles are exposed to the alternating magnetic field. Only a certain amount of drugs can be carried and released by a magnetic nanoparticle [18]. Mesoporous silica has gotten a lot of attention in drug loading and release due to its larger pore volume and size. Mesoporous silica's higher toughness, biocompatibility, surface functionalization, higher efficiency of cellular internalization makes an excellent candidate for use as super magnetic nanoparticles coating in drug distribution and delivery [19]. Furthermore, due to iron oxide composition, such mesostructured is particularly distinctive for clinical applications in terms of toxicity, stability, and biocompatibility [20].

This research work describes the biocompatible inorganic nanoparticle synthesis by the sol-gel method used for the delivery of therapeutic hydrophobic anticancer drugs on the human cancer cell. Magnetic manipulation was achieved by incorporating superparamagnetic iron oxide nanocrystals into mesoporous silica nanoparticles. Chemotherapeutic drug molecules were packed into the mesoporous silicate pores and subsequently delivered into PANC-1 cell lines to improve the therapeutic efficiency, reduced the conventional chemotherapy side effects, and overcoming the insolubility problem of hydrophobic drugs. The anticancer drug-loaded $\text{Fe}_3\text{O}_4@/\text{SiO}_2$ core/shell nanoparticles system developed in this study could pave the way for in vivo selective and controlled cancer therapeutics.

2. MATERIAL AND METHODS

$\text{Fe}(\text{acac})_3$, (97%), 1, 2-dodecanediol (92%), oleic acid (90%), oleylamine (70%), benzyl ether (98%), hexane (98.5+%), hexadecyltrimethylammonium bromide (CTAB, 99+%), tetraethyl orthosilicate (TEOS, 98%), phosphate-buffered saline (PBS,

10 \times), Paclitaxel and Camptothecins purchased from Cayman Chemical, Dimethyl sulfoxide (DMSO, 99.9+%), sodium hydroxide (NaOH, 97+%), hydrochloric acid (HCl, 36.5% 38%, trace metal grade) purchased from Fisher Scientific. Dulbecco's modified Eagle medium (DMEM) with high glucose, fetal bovine serum (FBS), antibiotics (10, 000 U/mL penicillin, 10, 000 $\mu\text{g}/\text{mL}$ streptomycin, and 29.2 mg/ mL L-glutamine), trypsin-ethylenediaminetetraacetic acid (trypsin-EDTA) (0.05%) were purchased from Gibco and Dulbecco's phosphate-buffered saline (DPBS). Cell-counting kit-8 (CCK-8) was purchased from Dojindo Molecular Technologies, Inc. Ethanol (200 proof) was purchased from Decon Laboratories, Inc.

2.1 Synthesis of Fe_3O_4 Nanoparticles

Under nitrogen flow, $\text{Fe}(\text{acac})_3$ (2 mmol), 1,2 hexadecanediol (10 mmol), oleic acid (6 mmol), oleylamine (6 mmol), and benzyl ether (15 mL) were combined and magnetically stirred. Under a nitrogen blanket, the reaction mixture was heated to reflux (363 $^\circ\text{C}$) for another 30 minutes after being heated to 298 $^\circ\text{C}$ for 30 minutes. The mixture was formulated into black-brown color and allowed to cool to room temperature. 40 mL ethanol was applied at room temperature, and black content was precipitated and centrifugated. In presence of hexane, a black material was dissolved in (0.05 ml) oleylamine and (0.05 ml) oleic acid. For solvent removal, centrifugation at 6000 rpm for 10 minutes was used, followed by dispersion in hexane [21].

2.2 Synthesis of $\text{Fe}_3\text{O}_4@/\text{MSNs}$ Nanoparticles

Fe_3O_4 nanoparticles (2.5 mg) were dispersed in 0.2 ml chloroform and added to 2 ml of 40 mg of CTAB in the Fe_3O_4 solutions. The reaction mixture was sonicated for 20 mins with a properly sealed cover to make oil in a water solution. The emulsion was then sonicated for 2 hrs. to evaporate the chloroform. A well-dispersed CTAB Fe_3O_4 aqueous solution (3 ml) was obtained. Then, in 18 ml of water 40 mg of CTAB was dissolved with 120 μl of 2 M NaOH solution in a 100 ml flask. At 70 $^\circ\text{C}$ and constant stirring, 2 ml of CTAB Fe_3O_4 aqueous solution was applied to the reaction solution. For mesoporous silica shell coating on CTAB Fe_3O_4 , add 1.2 ml ethyl acetate and 200 μl of TEOS dropwise in the solution and allowed it to stir for

2 hrs. After that solution was cooled, centrifuged and thrice times washed with ethanol. $\text{Fe}_3\text{O}_4@$ MSNs was distributed properly in ethanol (20 ml) contain 120 mg NH_4NO_3 , and to remove surfactants stirred at 60°C for 1hr. To make surfactant-free nanoparticles, the surfactant removal process was repeated two times and $\text{Fe}_3\text{O}_4@$ MSNs nanoparticles were washed multiple times with distilled water and ethanol [22].

2.3 Characterization

The size and morphology of nanoparticles were determined using transmission electron microscopy (TEM, Tecnai T12). In ethanol, Fe_3O_4 and $\text{Fe}_3\text{O}_4@$ MSNs nanoparticles were dispersed. The suspension of nanoparticles was placed onto a carbon-coated grid and allowed to dry at room temperature [23].

2.4 Magnetic Hyperthermia Experiment

Using an alternating magnetic (AM) current hyperthermia experiment with a magnetic field power of $H=180$ Gauss and a frequency of $F=409$ kHz, the magnetic heating efficiency of Fe_3O_4 nanoparticles was evaluated. 2 mg, 4 mg, and 6 mg/ml Fe_3O_4 nanoparticles were distributed in toluene and mounted in the coil center for this experiment. A thermocouple was used to continuously record thermal response data while the magnetic field was applied [24].

2.5 Loading Capacity Analysis of Paclitaxel (PTX) and Camptothecin (CPT) on $\text{Fe}_3\text{O}_4@$ MSNs nanoparticles

$\text{Fe}_3\text{O}_4@$ MSNs nanoparticles were loaded with 20 mM Paclitaxel (PTX) and 40 mM Camptothecin (CPT) and washed with water five times and PBS 7 times. The supernatant was collected at each washing step and absorption was measured by U.V-visible spectroscopy (Cary 5000). To calculate the amount of drug loading was calculated by loading capacity: (loaded drug mass divided by particles mass) $\times 100$ [25].

2.6 Drug Release Efficiency of Paclitaxel (PTX) and Camptothecin (CPT) $\text{Fe}_3\text{O}_4@$ MSNs nanoparticles

Release efficiency of Paclitaxel (PTX) and Camptothecin (CPT) $\text{Fe}_3\text{O}_4@$ MSNs (0.05 mg)

nanoparticles in 1ml of PBS was put in a hot water bath at a different temperature like 23°C, 37°C, 50°C, 80°C with their controls.

Release efficiency of Paclitaxel (PTX) and Camptothecin (CPT) $\text{Fe}_3\text{O}_4@$ MSNs nanoparticles (0.05 mg/ml) was evaluated by using an alternating magnetic field (AMF) with a magnetic field power of $H=180$ Gauss and a frequency of $F=409$ kHz. Centrifugation (7930 rpm, 20 min) was used to separate PTX and CPT released from nanoparticles, which were then measured using UV-visible spectrophotometry (Cary 5000). PTX and CPT release efficiencies are described as the released cargo mass divided by loaded cargo mass multiplied by 100 percent [25].

2.7 Cell Viability Assay

Human cancer cell lines (PANC-1) were supplied by the American Type Culture Collection. Cell culture media were prepared and changed after three days. Cells were passaged using trypsinization until confluence [26].

A cell-counting kit-8 assay was used to find PANC-1 viability after treated with Paclitaxel (PTX) and Camptothecin (CPT) $\text{Fe}_3\text{O}_4@$ MSNs nanoparticles with their controls. The cells were seeded at a density of 5×10^3 cells in DMEM for 24 hrs. The medium was removed, and the cells were incubated for 24 hrs in 200 L of fresh DMEM containing Paclitaxel (PTX) and Camptothecin (CPT) $\text{Fe}_3\text{O}_4@$ MSNs nanoparticles (i.e., 0, 75, and 100 $\mu\text{g}/\text{mL}$). To determine cell viability, each well was filled with DMEM and CCK-8 (10 ml) cellular cytotoxicity reagent and placed in the incubator. Tecan M1000 plate reader was used to test the absorbance at 450 and 650 nm to determine the number of viable cells [26].

3. RESULTS AND DISCUSSIONS

3.1 Production and Characterization of Fe_3O_4 and $\text{Fe}_3\text{O}_4@$ MSNs Nanoparticles

Fe_3O_4 nanoparticles are formed when $\text{Fe}(\text{acac})_3$ reacts with surfactants at high temperatures and is separated from reaction byproducts and high boiling point benzyl ether. Fe_3O_4 nanoparticles of 8-12 nm were formed when benzyl ether was used as the solvent. The large size Fe_3O_4 nanoparticles

obtained from benzyl ether seem to show that a higher reaction temperature would result in larger particles. The key for Fe_3O_4 nanoparticles production is to heat the mixture to 298°C for 30 mins and then reflux at 363°C . A broad range of Fe_3O_4 nanoparticles from 8 to 12 nm are synthesized indicating that Fe_3O_4 nuclei growth is not a quick process under these reaction conditions (Fig 1).

Long-chain alcohols, such as 1,2 hexadecanediol, have been discovered to react well with $\text{Fe}(\text{acac})_3$ to form Fe_3O_4 nanoparticles of large size. The reaction produces a red-brown product due to the use of oleic acid. The reaction mixture with only oleylamine produces far fewer Fe_3O_4 nanoparticles than the reaction with both Oleic acid and oleylamine. As particles are oxidized at room temperature by bubbling oxygen by dispersion, they are further precipitated. Increasing the amount of oleylamine results in a redder brown product dispersion. Nanoparticles with a cargo-carrying capacity made with a mesoporous silica shell around a superparamagnetic Fe_3O_4 core [27].

The mechanism for the synthesis of iron oxide nanoparticles is based on the condensation process that occurs during the colloidal growth process. The atomic species that make up an iron oxide particle are stacked on top of each other. The partial reduction and breakdown of $\text{Fe}(\text{oleate})_3$ in the presence of oleylamine produces these atomic species. The clustering of the "Fe-O" species produces many nuclei that are saturated in the reaction media and assemble into iron oxide nanoparticles [28]. The solubility of the nuclei in the dispersion determines when nucleation ceases and nuclei aggregation takes control of the growth process. If the nuclei in the dispersion medium are not saturated, the particles cannot develop. The nuclei aggregation becomes impulsive over the saturation threshold till the particles are heated from the dispersion. The reduction in solvent volume in the production of Fe_3O_4 nanoparticles causes early saturation of the oxide-based nucleus, allowing more reactants to participate in the growth cycle, resulting in bigger particles [29]. However, in a greater volume solvent, more nuclei are required to reach saturation, which comes at the expense of the iron salt precursor, leading to reduced Fe_3O_4 nanoparticles. A similar idea can be applied to the surfactant phenomenon. In a high surfactant/metal ratio, more surfactant equates to a larger volume

of solvent, and more nuclei are required to reach saturation, resulting in small nanoparticles [30].

Surfactant coating was attained by condensation and hydrolysis of tetraethyl orthosilicate (TEOS) in the presence of hexadecyltrimethylammonium bromide (CTAB). The diameter of Fe_3O_4 @MSN nanoparticles was determined to be 90 nm to 110 nm using Transmission electron microscopy (TEM) (Fig 2).

In a mixture of ethanol, H_2O , CTAB, and ammonium hydroxide, alkoxy silane undergoes hydrolysis and condensation processes, resulting in mesoporous silica. The interaction between the nucleation (hydrolysis) and growth (condensation) processes is critical for efficient encapsulation of the mesoporous silica shell on the Fe_3O_4 core. When the condensation rate exceeds the hydrolysis rate, silica is vulnerable to encapsulating Fe_3O_4 nanoparticles. During the production of the mesoporous silica shell, CTAB works as a surfactant as well as a structure-directing agent. To produce spherical micelles, CTA^+ cations first form tight bonds with negative charge Fe_3O_4 nanoparticles. Electrostatic attraction attracts the silicon oligomers produced by TEOS to the spherical micelles [31]. At low concentrations, unbound silicon oligomers primarily deposit on micelle- Fe_3O_4 nanoparticle junctions to conceal the electrostatic repulsion between adjoining head groups in micelles. Furthermore, ethanol diffusion inhibits alkyl tail self-interaction in CTAB micelles, boosting hydrophobic volume and decreasing spherical micelle curvatures. Moreover, using ammonium hydroxide as a basic catalyst can help create hydrogen bonds between neighbouring CTAB micelles and silicon oligomers, promoting the creation of parallel mesoporous channels and lowering micelle curvature energy. Consequently, CTAB-silicon oligomers are structurally transformed from spherical to cylindrical forms. As a consequence, of the above four ingredients, newly hydrolyzed silicon oligomers are adsorbed on the silica/solution interface area and can be further cross-linked via charged head groups. As a result, continuous mesopores form in the axial direction of cylindrical micelles parallel to the nanoparticle surface [28-33].

3.2 Iron oxide Nanoparticles Triggered by Alternating Magnetic field (AMF)

Iron oxide (Fe_3O_4) nanoparticles were distributed

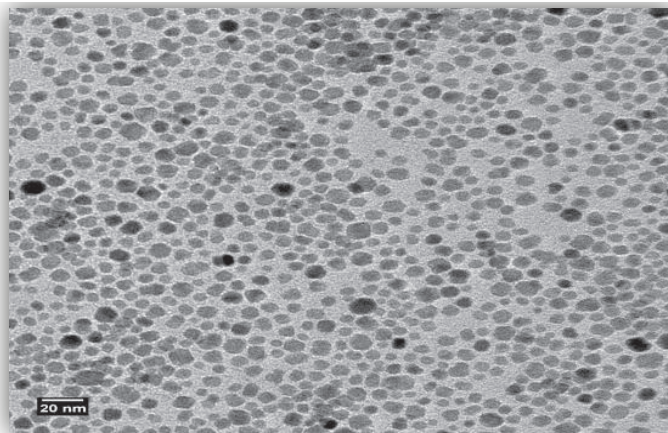


Fig.1. TEM images of Fe_3O_4 produced nanoparticles

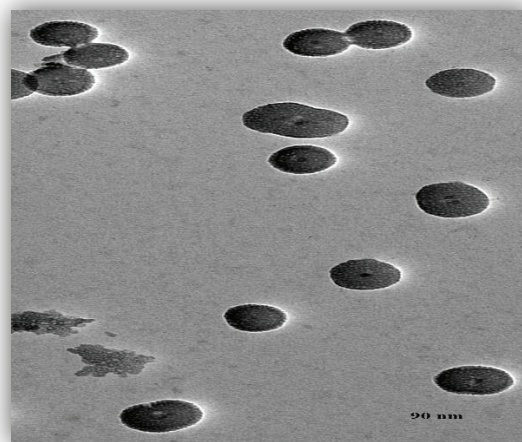
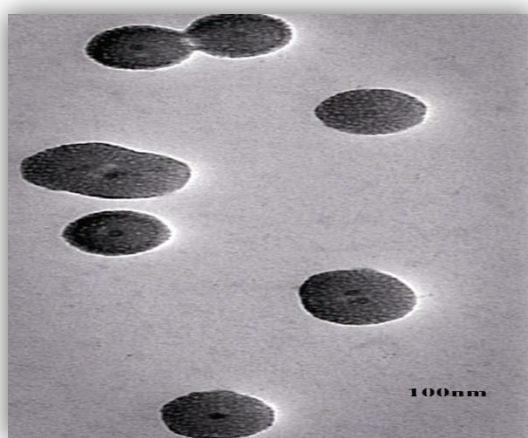


Fig. 2. TEM illustrations of Fe_3O_4 @MSNs nanoparticles

in toluene and for heat production, an alternating magnetic field (375 kHz, 5 kW) was used. Fig 3 showed an increase in the temperature profile of time and concentration-dependent when the AMF trigger was applied. The temperature of the toluene solution containing 2mg/ml, 4mg/ml, and 6mg/ml nanoparticles finally achieved 30°C, 33°C, and 35°C after 300 secs.

The ability of Fe_3O_4 nanoparticles to heat up when exposed to AMF shows that they could be used as a heat source for thermally induced drug release. AMF may be responsible for the core and shell mechanism. If movement induced by AMF is confirmed, there is a Brownian heating mechanism of the Fe_3O_4 core in mesoporous silica nanoparticles. In the presence of AMF, there were two probable core moments. 1) Neel relaxation process in which the iron core does not reorient in the AMF, requiring the formation of a dipole atomic structure in the iron core to raise the temperature.

2) The iron core oscillation in the AMF drive silica shell is the other mechanism at work. This resulted in a rise in temperature due to friction-induced by iron mesoporous core-shell nanoparticles, indicating that Brownian relaxation plays a role in the temperature shift of the nano environment [34].

3.3 Loading Capacity Analysis of PTX and CPT Fe_3O_4 @MSNs Nanoparticles

To realize the loading of PTX and CPT on Fe_3O_4 @MSNs nanoparticles using ethanol and DMSO, widely used solvents for poorly water-soluble drugs. PTX and CPT loading onto Fe_3O_4 @MSNs nanoparticles was achieved by soaking overnight and then after 24 hrs loaded nanoparticles were introduced back to the aqueous solution. To calculate the loading capacity by definition as (loading drug mass divided by particles mass) \times 100. The drug-loaded nanoparticles were washed with ethanol and DMSO at different times until the supernatant

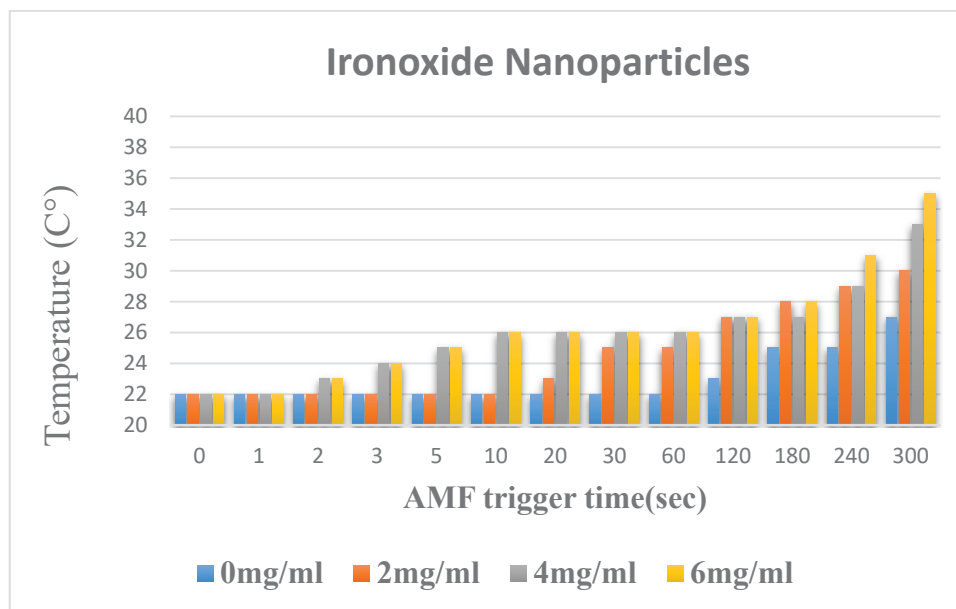


Fig. 3. The temperature increase profile of iron oxide nanoparticles enabled by AMF is time and temperature-dependent.

after centrifugation was clear and collected using U.V-visible spectroscopy. Loading capacity was achieved 20 mM of Paclitaxel was 6.2% and 40 mM of Camptothecin was 8% respectively. $\text{Fe}_3\text{O}_4@\text{MSNs}$ nanoparticles drug loading capacity is due to the mesoporous silica's increased surface area, which provides additional interior spaces and conjugation sites.

The magnetic hollow porous nanocrystal shells have a very high paclitaxel (PTX) loading (20.2 percent) capacity [35]. Sahu and colleagues developed a multimodal theranostic nanoagent based on hollow magnetic mesoporous silica as an effective carrier for high loading and regulated release of Camptothecin (CPT). The synthesized nanomagnetic carrier had a drug-loading capacity of 17.5% [36].

3.4 Influence of External Heating / Oscillating Magnetic Field on PTX and CPT Release from $\text{Fe}_3\text{O}_4@\text{MSNs}$ Nanoparticles

Samples tubes contain PTX and CPT $\text{Fe}_3\text{O}_4@\text{MSNs}$ nanoparticles (0.05 mg/ml) dispersed in deionized water were put in a hotplate of water bath set at 37, 50, and 80°C for 60, 120, 180, and 240 min known as bulk heating. To collect untrapped drug molecules, PTX and CPT loaded $\text{Fe}_3\text{O}_4@\text{MSNs}$

nanoparticles were washed in PBS buffer. The supernatant was collected after the samples were heated and spun down for release calculation. As a control, a non-heated sample at 23 °C was used. The release efficiency is calculated as (the mass of the leaked drug divided by the mass of the loading drug) divided by 100. After 60 mins of heating at a higher temperature (80°C), 70% of the PTX was released with a release efficiency of 70%. Furthermore, 73 and 76% of the drug were released after 120 and 180 min of heating at 80°C, respectively. Nearly 80% of the drug was released at (80°C) after 240 minutes. On the other hand, the release efficiency of the drug at 37°C and 50°C at 240 min is 49% and 62% respectively. The control group at 23 °C drug leakage is only 7.8% at 240 min Fig 4(a). This indicates that the drug was successfully constructed on the surface of $\text{Fe}_3\text{O}_4@\text{MSNs}$ nanoparticles, as shown by the presence of premature leakage at room temperature or physiological temperature. It can simply be inferred that the amount of cargo released is determined by the temperature of the water bath.

$\text{Fe}_3\text{O}_4@\text{MSNs}$ nanoparticles are loaded with the drug Camptothecin. These solid particles showed no drug release at 0 min. When the solution was heated up to 80°C by external hotplate heating at various time intervals for 60, 120, 180, and 240 min there

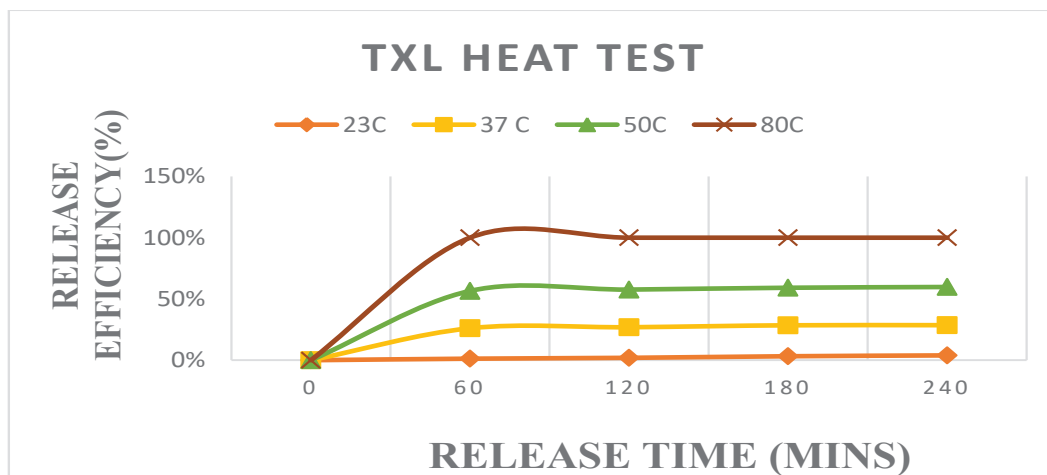


Fig. 4(a). External heating for 1, 2, 3, and 4 hours provided a time dependents leakage profile of Paclitaxel (PTX) from Fe_3O_4 @MSNs nanoparticles in PBS buffer.

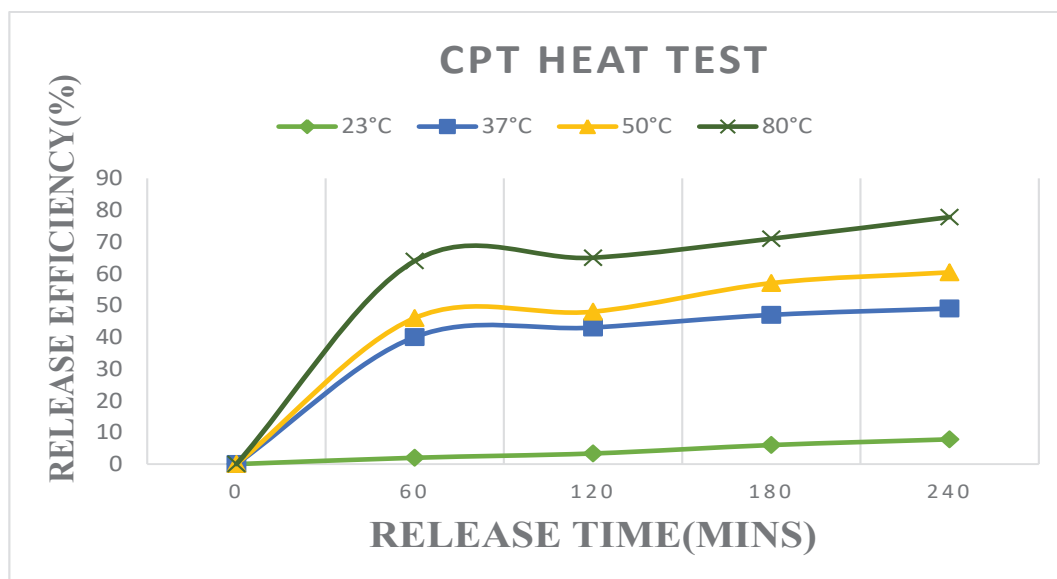


Fig. 4(b). External heating for 1, 2, 3, and 4 hours developed a time dependents leakage profile of Camptothecin (CPT) from Fe_3O_4 @MSNs nanoparticles in PBS buffer.

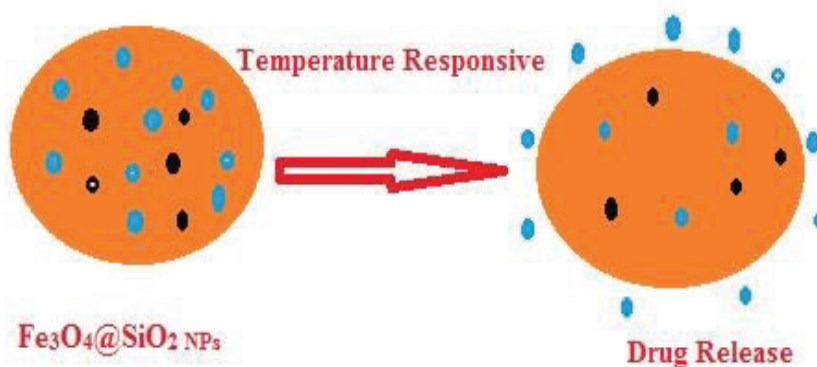


Fig. 4 (c). Scheme illustration of drug release after temperature stimulus-response

was an increase in drug release efficiency was 64%, 65%, 71%, and 77.8% respectively as shown in Fig 4(b). The release efficiency of the drug at 37°C at 240 min is 49%. The control group at 23°C drug leakage is only 7.8% at 240min. The sample heated at (50°C) for 60, 120, 180, and 240 mins and the drug leakage efficiency was 46%, 48%, 57% 60.4% respectively. Both these release results indicate that heating itself can help in drug release (37 - 80°C). Fig 4(c) determines that temperature has a great impact on the molecule's thermodynamic behavior. By increasing the bulk solution temperature to find out that if an increase of surrounding temperature will trigger drug release.

Super magnetic iron oxide nanoparticles were induced at huge temperatures when exposed to the alternating magnetic field. After coated with a mesoporous silica shell, magnetic Fe₃O₄@MSNs increases the local and surrounding temperature to various extents depending upon the alternating magnetic field intensity and as well particle size. For various lengths of time, an alternating magnetic field (AMF) is used as an internal heat resource for drug leakage. PTX and CPT Fe₃O₄@MSNs nanoparticles were distributed at room temperature in PBS (0.05 mg/mL). To confirm the drug leakage before triggering with magnetic heating was monitored by centrifugation of nanoparticles and separate the supernatant observed under U.V- visible spectrophotometer. The sample was mounted in a 3 turn copper coil that was water-cooled and capable of producing an alternating magnetic field (AMF) with a power of 5kW and a frequency of 375 kHz. The exposure time applied was 30 mins, 60 mins, 120 mins, and 180 mins. Only slight leakage was observed. The uptake and as well release efficiency of PTX and CPT Fe₃O₄@MSNs core/shell nanoparticles are lower because of the radial porous size structure instead of a 2D hexagonal array with a central pore occupied by Fe₃O₄ and oleic acid as the stabilizing agent covers the iron oxide [37].

Comparing this experiment with external heating it was found that nanoparticle local temperature is much lower than doesn't supply enough energy to release the cargo.

3.5 *In vitro* Studies of Cytotoxicity

Many anticancer medications have low water

solubility, making intravenous administration difficult. As a result, developing novel delivery mechanisms for these drugs that do not rely on organic solvents is crucial for cancer treatment. In this, we determine the hydrophobic drug-delivery system's potential biological applications, *in vitro* cytotoxicity tests were performed. Using PTX and CPT Fe₃O₄@MSNs nanoparticles, the cytotoxicity of a pancreatic cancer cell line was assessed using a colorimetric cell counting kit-8 (CCK-8) assay.

To assess PTX Fe₃O₄@MSNs nanoparticles toxicity on PANC-1, cell culture experiments were performed by CCK-8 assay. With each increase in nanoparticle concentration, cell viability decreased in a dose-dependent manner. PTX Fe₃O₄@MSNs nanoparticles at the maximum concentration of 100ug/ml demonstrated substantial cytotoxicity, decreasing cell survival to 25% ± 3.9, whereas the control group had no significant decrease in viable cell numbers. In comparison to the control (Fe₃O₄@MSNs nanoparticles), low doses of PTX Fe₃O₄@MSNs nanoparticles (75 ug/ml) tend to demonstrate substantial cytotoxicity 41% ± 2.9. The results showed that PTX Fe₃O₄@MSNs nanoparticles can significantly reduce cell viability Fig 5(a).

CCK8 assay relative percentage viability was determined at selected CPT Fe₃O₄@MSN's nanoparticles concentrations with standard deviations. Among selected in a CCK-8 assay-based cell viability study revealed that CPT Fe₃O₄@MSNs nanoparticles on PANC-1 cells showed viability percentage cytotoxicity at 100 and 75 ug/ml concentration Fig 5(b). At 100 µg/ml concentration CPT Fe₃O₄@MSN's nanoparticles cell viability percentage (25% ± 3.2) after 24 hrs.

PTX and CPT Fe₃O₄@MSNs nanoparticles were uptaken by PANC-1 cells, and the drug was released from nanocarriers in PANC-1 cells, according to these findings. These findings strongly suggest that PANC-1 cells ingested NPs with a high PTX/CPT ratio. Since NPS comes into contact with the acidic and redox microenvironment in tumor cells, hydrophobic drugs are released quickly. Caveolae-mediated endocytosis allowed PTX and CPT Fe₃O₄@MSN nanoparticles to reach PANC-1 cells [38 - 40]. As a result, these findings strongly suggested that PTX and CPT Fe₃O₄@MSN nanoparticles loaded and delivered successfully into pancreatic cancer cells and decreased cancer cell

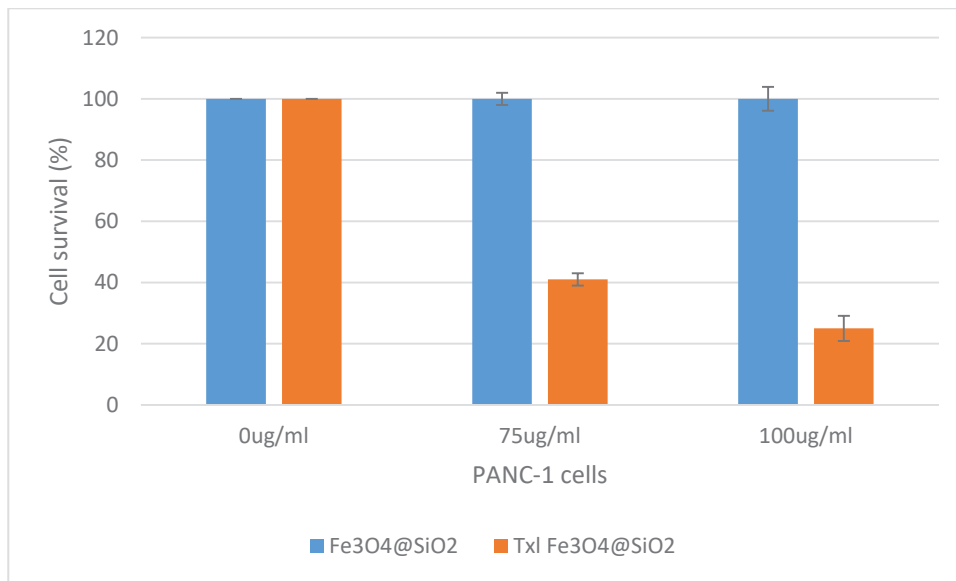


Fig. 5(a). PANC-1 cell viability after exposure to PTX Fe_3O_4 @MSN nanoparticles. The data are the averages of three separate experiments plus or minus the standard deviation.

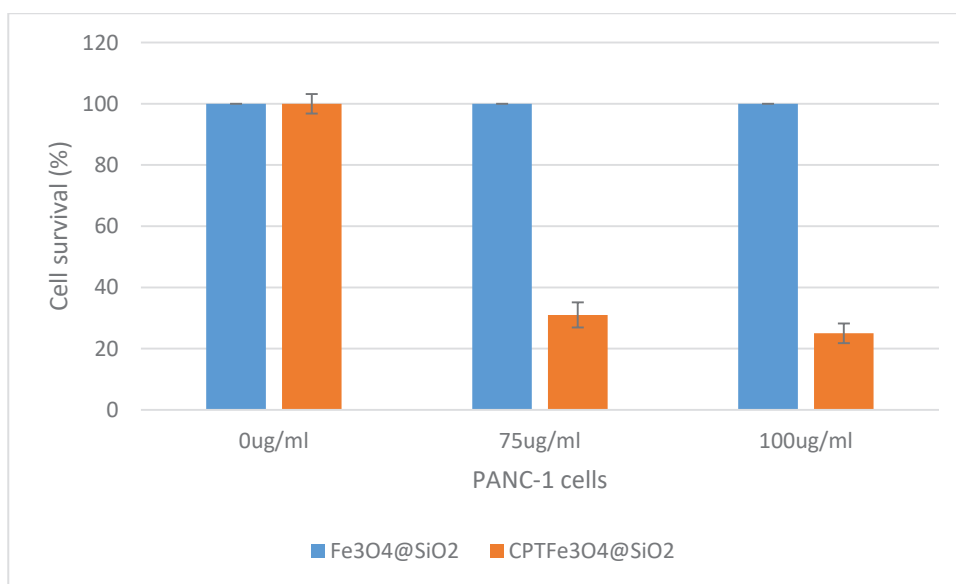


Fig. 5(b). PANC-1 cell viability after being treated with CPT Fe_3O_4 @MSN nanoparticles. The results are based on three separate experiments. Standard deviations are represented by error bars.

viability. According to the study, the cytotoxicity of Fe_3O_4 @MSN loaded with the chemotherapeutic drug Paclitaxel is significantly higher than that of magnetic nanoparticles containing only Fe_3O_4 . The slower drug release of PTX from the porous shell channels of the magnetic hollow porous nanocrystal shells explains the anticancer efficacy of the nanoparticles [35]. A multimodal

theranostic nanoagent based on Camptothecin (CPT) loaded magnetic mesoporous silica are not only exceptionally durable in aqueous buffer, but also have a high level of cytotoxicity via apoptosis induction [36]. It would be fascinating to see if this approach can be applied to other anticancer medications. Since water insolubility of therapeutic anticancer drugs is a common issue in successful

cancer therapy development, our research suggests that mesoporous silica nanoparticles are a good solution.

4. CONCLUSION

We successfully synthesized inorganic, biocompatible core/shell structured superparamagnetic iron oxide nanocrystals encased within mesostructured silica spheres as proof of a viable platform for simultaneous hydrophobic drug delivery. To investigate drug loading and release profiles, the pores of $\text{Fe}_3\text{O}_4@\text{MSN}$ nanoparticles are saturated with hydrophobic drugs such as Paclitaxel and Camptothecin. In comparison, to the alternating magnetic field (AMF), which does not generate adequate heat, thermal heating helps to release the hydrophobic drugs from $\text{Fe}_3\text{O}_4@\text{MSN}$ nanoparticles pores. PTX and CPT $\text{Fe}_3\text{O}_4@\text{MSN}$ nanoparticles perform as valuable drug delivery vehicles and cancer-targeting mediators, boosting the death of PANC-1 cancer cells. PTX and CPT $\text{Fe}_3\text{O}_4@\text{MSNs}$ nanoparticle-based targeted drug delivery may be effective in treating PANC-1 cancer cells while minimizing toxicity to normal tissues in the surrounding region. These nanoparticles may be useful for successful drug delivery vehicles because of the simple procedures and targeting aspect.

5. ACKNOWLEDGEMENTS

The experimental procedures are undertaken in this project were financially supported by the Higher Education Commission of Pakistan under the IRSIP program.

6. REFERENCES

1. O.C. Farokhzad., J. M. Karp., and R. Langer. Nanoparticle-aptamer bioconjugates for cancer targeting. *Expert Opinion on Drug Delivery* 3 :311-24 (2006)
2. F. S. Collins, and H. A. Varmus. New Initiative on Precision Medicine. *The New England Journal of Medicine* 372: 793–795 (2015)
3. E.M. Alexandrino, S. Ritz, F. Marsico, G. Baier, V. Mailänder, K. Landfester. Paclitaxel-loaded polyphosphate nanoparticles: a potential strategy for bone cancer treatment. *Journal of Materials Chemistry B* 2 : 1298-1306 (2014)
4. M. Wu, X.M. Xia, C. Cui, P. Yu, Y. Zhang, and L. Liu., Highly efficient loading of amorphous paclitaxel in mesoporous hematite nanorods and they are in vitro antitumor activity. *Journal of Materials Chemistry* 1: 1687-1695 (2013)
5. K.S. Cunha, M.L. Reguly, U. Graf, and H. H. Rodrigues de Andrade. Comparison of camptothecin derivatives presently in clinical trials: genotoxic potency and mitotic recombination. *Mutagenesis* 17(2): 141-7 (2002).
6. M. Duphal, and D. Chowdry. Phytochemical-Based Nanomedicine for Advanced Cancer Theranostics: Perspectives on Clinical Trials to Clinical Use. *International Journal of Nanomedicine* 15: 9125-9157 (2020)
7. R.W. Peck, Precision Medicine Is Not Just Genomics: The Right Dose for Every Patient. *Annual Review of Pharmacology and Toxicology* 58: 105–122 (2018)
8. Z. Li, D.L. Clemens, B.Y. Lee, B. J. Dillon, M. A. Horwitz, and J.I. Zink. Mesoporous Silica Nanoparticles with pH-Sensitive Nanovalves for Delivery of Moxifloxacin Provide Improved Treatment of Lethal Pneumonic Tularemia. *American Chemical Society Nano* 9 : 10778–10789 (2015)
9. B. Ruehle, D.L. Clemens, B.Y. Lee, M.A. Horwitz, and J. I. Zink. A Pathogen-Specific Cargo Delivery Platform Based on Mesoporous Silica Nanoparticles. *The Journal of the American Chemical Society* 139 : 6663–6668 (2017)
10. R. Mo, T. Jiang, R. Disanto, W. Tai, and Z. Gu, ATP-Triggered Anticancer Drug Delivery. *Nature Communications* 5: 3364 (2014) DOI: 10.1038/ncomms4364
11. H. Li, L.L. Tan, P. Jia, Q.L. Li, Y.L. Sun, J. Zhang, Y.Q. Ning, J. Yu, and Y.W. Yang. Near-Infrared Light-Responsive Supramolecular Nanovalve Based on Mesoporous Silica-Coated Gold Nanorods. *Chemical Science Journal* 5: 2804–2808 (2014).
12. Y. Zhu and C. Tao. DNA-Capped $\text{Fe}_3\text{O}_4/\text{SiO}_2$ Magnetic Mesoporous Silica Nanoparticles for Potential Controlled Drug Release and Hyperthermia. *RSC Advances* 5: 22365–22372 (2015)
13. J. L. Paris, M. V. Cabanas, M. Manzano, and M. Vallet-Regí. Polymer-Grafted Mesoporous Silica Nanoparticles as Ultrasound Responsive Drug Carriers. *American Chemical Society Nano* 9: 11023–11033 (2015)
14. M. De. Smet, E. Heijman, S. Langereis, N. M. Hijnen, and H. Grüll. Magnetic Resonance Imaging of High Intensity Focused Ultrasound Mediated Drug Delivery from Temperature-Sensitive Liposomes:

- An in Vivo Proof-of-Concept Study. *The Journal of Controlled Release* 150: 102–110 (2011)
15. X. Huang, I. H. El-Sayed, W. Qian, M. and A. El-Sayed, Cancer Cell Imaging and Photothermal Therapy in the Near-Infrared Region by Using Gold Nanorods. *The Journal of the American Chemical Society* 128 : 2115–2120 (2006)
 16. R. Nicola, O. Costișor, S. Muntean, M. Nistor, A. Putz, C. Ianăși, R. Lazău, L. Almásy, and L. Săcărescu. Mesoporous magnetic nanocomposites: a promising adsorbent for the removal of dyes from aqueous solutions. *Journal of Porous Materials* 27: 413–428 (2020)
 17. J. F. Liu, B. Jang, D. Issadore, and A. Tsourkas. Use of Magnetic Fields and Nanoparticles to Trigger Drug Release and Improve Tumor Targeting. *Nanomedicine and Nanobiotechnology* 11(6): e1571 (2019) doi:10.1002/wnan.
 18. Z. Medarova, W. Pham, C. Farrar, V. Petkova, and A. Moore. In-Vivo Imaging of siRNA Delivery and Silencing in Tumors. *Nature Medicine* 13 : 372–377 (2007)
 19. K. Boubbou, R. Ali , S. Al-Humaid , A. Alhallaj, O. M. Lemine, M. Boudjelal , and A. AlKushi. Iron Oxide Mesoporous Magnetic Nanostructures with High Surface Area for Enhanced and Selective Drug Delivery to Metastatic Cancer Cells. *Pharmaceutics* 13: 553 (2021) <https://doi.org/10.3390/pharmaceutics13040553>
 20. F. Ahmadpoor, A. Masood, N. Feliu, W. J. Parak, and S. A. Shojaosadati. The Effect of Surface Coating of Iron Oxide Nanoparticles on Magnetic Resonance Imaging Relaxivity. *Frontier in Nanotechnology* 3:644- 743(2021)
 21. T. Xia, M. Kovichich, M. Liang, H. Meng, S. Kabehie, S. George, J. I. Zink, and A. E. Nel, Polyethyleneimine Coating Enhances the Cellular Uptake of Mesoporous Silica Nanoparticles and Allows Safe Delivery of siRNA and DNA Constructs. *American Chemical Society Nano* 3 : 3273–3286 (2009)
 22. S. Wu, H. C. Y. Lin, Y. Hung, W. Chen, C. Chang, and C. Y. Mou. PEGylated Silica Nanoparticles Encapsulating Multiple Magnetite Nanocrystals for High-Performance Microscopic Magnetic Resonance Angiography. *Journal of Biomedical Materials Research - Part B Applied Biomaterials* 99B: 81–88 (2011)
 23. P. Saint-Crick, S. Deshayes, J. I. Zink, and A. M. Kasko. Magnetic Field Activated Drug Delivery Using Thermodegradable Azo-Functionalised PEG-Coated Core-Shell Mesoporous Silica Nanoparticles. *Nanoscale* 7 (31): 13168– 13172 (2015) DOI: 10.1039/C5NR03777H
 24. A. Baeza, E. Guisasola, E. Ruiz-Hernández, and M. Vallet-Regí. Magnetically Triggered Multidrug Release by Hybrid Mesoporous Silica Nanoparticles. *Chemistry of Materials* 24 (3):517– 524 (2012) DOI: 10.1021/cm203000
 25. X. Liu, Y. Zhang, Y. Wang, W. Zhu, G. Li, X. Ma, Y. Zhang, S. Chen, S. Tiwari, K. Shi, S. Zhang, H. M. Fan, Y. X. Zhao, and X-J. Liang. Comprehensive Understanding of Magnetic Hyperthermia for Improving Antitumor Therapeutic Efficacy. *Theranostics* 10 (8): 3793– 3815 (2020) DOI: 10.7150/thno.40805
 26. A. P. Katsoulidis, D. E. Petrakis, G. S. Armatas, and P. J. Pomonis. Microporosity, pore anisotropy and surface properties of organized mesoporous silicates (OMSi) containing cobalt and cerium. *The Journal of Materials Chemistry* 17: 1518–1528 (2007)
 27. X. Yu, P. Kaithal, H. Luo, P. Soman, and S. Ramakrishna, Magnetic Iron Oxide Nanoparticle (IONP) Synthesis to Applications: Present and Future. *Materials*, 13:4644 (2020) doi:10.3390/ma13204644
 28. C. Hui, C. Shen, J. Tian, L. Bao, H. Ding, C. Li, Y. Tian, X. Shiab, and H. Gao, Core-shell Fe₃O₄@SiO₂ nanoparticles synthesized with well-dispersed hydrophilic Fe₃O₄ seeds. *Nanoscale* 3: 701–705 (2011)
 29. U. Klekotka, D. Satuła , A. Basa, and B. Kalska-Szostko, Importance of Surfactant Quantity and Quality on Growth Regime of Iron Oxide Nanoparticles. *Materials* 13: 1747 (2020) doi:10.3390/ma13071747
 30. C. K. Dixit, S. Bhakta, A. Kumar, S. L. Suib , and J. F. Rusling. Fast nucleation for silica nanoparticle synthesis using a sol-gel method. *Nanoscale* 1;8(47):19662-19667 (2016). doi: 10.1039/c6nr07568a.
 31. W. Chen, F. Lu, C. C. V. Chen, K. C. Mo, Y. Hung, Z. X. Guo, C. H. Lin, M. H. Lin, Y. H. Lin, C. Chang, and C. Y. Mou. Manganese-Enhanced MRI of Rat Brain Based on Slow Cerebral Delivery of Manganese (II) with Silica-Encapsulated MnFe₁XO Nanoparticles. *NMR in Biomedicine* 26:1176–1185 (2013).
 32. X. Liu, Y. Zhang, Y. Wang, W. Zhu, G. G. Li, X. Ma, Y. Zhang, S. Chen, S. Tiwari, K. Shi, S. Zhang, H. Fan, M. Zhao, and Y. X. Liang. Comprehensive Understanding of Magnetic Hyperthermia for

- Improving Antitumor Therapeutic Efficacy. *Theranostics* 10 (8) : 3793– 3815 (2020) DOI: 10.7150/thno.40805
33. J. R. H. Manning, C. Brambila, and S. V. Patwardhan. Unified mechanistic interpretation of amine-assisted silica synthesis methods to enable design of more complex materials. *Molecular Systems Design & Engineering* 6: 170-196 (2021)
34. B. Luo, S. Xu, W.F. Ma, W.-R. Wang, S.L. Wang, J. Guo, W.L. Yang, J.H. Hu and C.C. Wang, Development of redox/pH dual stimuli-responsive MSP@P(MAA-Cy) drug delivery system for programmed release of anticancer drugs in tumour cells. *The Journal of Materials Chemistry* 20:7107–7113 (2010)
35. S. Sahu, N. Sinha, S. K. Bhutia, M. Majhi, and S. Mohapatra, Luminescent magnetic hollow mesoporous silica nanotheranostics for camptothecin delivery and multimodal imaging. *The Journal of Materials Chemistry* 2: 3799–3808 (2014)
36. H. L. Ding, Y. X. Zhang, S. Wang, J. M. Xu, and S. C. Xu, Fe₃O₄@SiO₂Core/Shell Nanoparticles: The Silica Coating Regulations with a Single Core for Different Core Sizes and Shell Thickness. *Chemistry of Materials* 24, 4572-4580 (2012) H.Lidx.doi.org/10.1021/cm302828d
38. J. Voigt, J. Christensen, and V. P . Shastri. Differential uptake of nanoparticles by endothelial cells through polyelectrolytes with an affinity for caveolae. *National Academy of Sciences (U.S.)* 111 (8) : 2942–7 (2014) DOI: 10.1073/pnas.1322356111
39. H. V. Quang, C. C. Chang, P. Song, E. M. Hauge, and J. Kjems. Caveolae-mediated mesenchymal stem cell labeling by PSS-coated PLGA PFOB nano-contrast agent for MRI. *Theranostics* 8(10): 2657-2671 (2018)
40. M. Mohammed, A. M Jawad, Z. Su, and C.Zhang. Stimuli-responsive Mesoporous silica nanoparticles for on-demand drug release. *International Journal of Advanced Research in Biological Sciences* 5(4): 152-166 (2018).